Constraints on the running of the running of the scalar tilt from CMB anisotropies and spectral distortions

Giovanni Cabass,[1] Eleonora Di Valentino,[2] Alessandro Melchiorri,[1] Enrico Pajer,[3] and Joseph Silk[2,4,5,6]

[1]*Physics Department and INFN, Università di Roma "La Sapienza", P.le Aldo Moro 2, 00185 Rome, Italy*
[2]*Institut d'Astrophysique de Paris (UMR7095: CNRS & UPMC-Sorbonne Universities), F-75014 Paris, France*
[3]*Institute for Theoretical Physics and Center for Extreme Matter and Emergent Phenomena, Utrecht University, Princetonplein 5, 3584 CC Utrecht, Netherlands*
[4]*AIM-Paris-Saclay, CEA/DSM/IRFU, CNRS, Univ. Paris VII, F-91191 Gif-sur-Yvette, France*
[5]*Department of Physics and Astronomy, The Johns Hopkins University Homewood Campus, Baltimore, Maryland 21218, USA*
[6]*BIPAC, Department of Physics, University of Oxford, Keble Road, Oxford OX1 3RH, United Kingdom*

(Received 15 May 2016; published 27 July 2016)

We use the recent observations of cosmic microwave background (CMB) temperature and polarization anisotropies provided by the Planck satellite experiment to place constraints on the running $\alpha_s = dn_s/d\log k$ and the running of the running $\beta_s = d\alpha_s/d\log k$ of the spectral index n_s of primordial scalar fluctuations. We find $\alpha_s = 0.011 \pm 0.010$ and $\beta_s = 0.027 \pm 0.013$ at 68% C.L., suggesting the presence of a running of the running at the level of two standard deviations. We find no significant correlation between β_s and foregrounds parameters, with the exception of the point sources amplitude at 143 GHz, A^{PS}_{143}, which shifts by a half-sigma when the running of the running is considered. We further study the cosmological implications of such a preference for $\alpha_s, \beta_s \sim 0.01$ by including in the analysis the lensing amplitude A_L, the curvature parameter Ω_k, and the sum of neutrino masses $\sum m_\nu$. We find that when the running of the running is considered Planck data are more compatible with the standard expectations of $A_L = 1$ and $\Omega_k = 0$ but still hint at possible deviations. The indication for $\beta_s > 0$ survives at two standard deviations when external data sets such as baryon acoustic oscillation surverys and CFHTLenS are included in the analysis and persists at ~1.7 standard deviations when CMB lensing is considered. We discuss the possibility of constraining β_s with current and future measurements of CMB spectral distortions, showing that an experiment like PIXIE could provide strong constraints on α_s and β_s.

DOI: 10.1103/PhysRevD.94.023523

I. INTRODUCTION

The recent measurement of the cosmic microwave background (CMB) anisotropies provided by the Planck satellite mission (see Refs. [1,2], for example) have provided a wonderful confirmation of the standard ΛCDM cosmological model. However, when the base model is extended and other cosmological parameters are let free to vary, a few "anomalies" are present in the parameter values that, even if their significance is only at the level of two standard deviations, deserve further investigation.

First of all, the parameter A_L, that measures the amplitude of the lensing signal in the CMB angular spectra [3], has been found larger than the standard value with $A_L = 1.22 \pm 0.10$ at 68% C.L. ($A_L = 1$ being the expected value in ΛCDM) from Planck temperature and polarization angular spectra [1]. A value of A_L larger than 1 is difficult to accommodate in ΛCDM, and several solutions have been proposed as modified gravity [4,5], neutrino anisotropies [6], and compensated isocurvature perturbations [7]. Combining Planck with data from the Atacama Cosmology Telescope and the South Pole Telescope to better constrain the foregrounds, Couchot *et al.* [8], found a consistency with $A_L = 1$. However, the compatibility of the CMB data sets used is unclear. More recently, Addison *et al.* [9] have found that including the A_L parameter solves the tension between Planck and WMAP9 on the value of the derived cosmological parameters.

As shown in Ref. [1], the A_L anomaly persists when the Planck data are combined with baryonic acoustic oscillation surveys (BAO), and it is enhanced when the CFHTLenS shear lensing survey is included, but it practically disappears when CMB lensing from Planck trispectrum observations are considered. The A_L anomaly is also still present in a 12-parameter extended ΛCDM analysis of the Planck data set (see Ref. [10]), showing no significant correlation with extra parameters such as the dark energy equation of state w, the neutrino mass, and the neutrino effective number $N_{\rm eff}$.

Second, the Planck data set prefers a positively curved universe, again at about two standard deviations with $\Omega_k = -0.040 \pm 0.020$ at 68% C.L. This anomaly is not due to an increased parameter volume effect, but, as stated in Ref. [2], curvature provides a genuine better fit to the data with an improved fit of $\Delta\chi^2 \sim 6$. When BAO data are included,

however, the curvature of the Universe is again compatible with zero with the stringent constraint $\Omega_k = -0.000 \pm 0.005$ at 95% C.L.

The fact that both the A_L and Ω_k anomalies disappear when reliable external data sets are included suggests that their origin might be a systematic or that they are produced by a different physical effect than lensing or curvature.

In this respect, it is interesting to note that a third parameter is constrained to anomalous values from the Planck data. The primordial scalar spectral index n_s of scalar perturbations is often assumed to be independent of scale. However, since some small scale-dependence is expected,[1] we can expand the dimensionless scalar power spectrum $\Delta^2_\zeta(k) = k^3 P_\zeta(k)/2\pi^2$ as

$$\Delta^2_\zeta(k) = A_s \left(\frac{k}{k_\star}\right)^{n_s - 1 + \frac{\alpha_s}{2}\log\frac{k}{k_\star} + \frac{\beta_s}{6}(\log\frac{k}{k_\star})^2}, \qquad (1)$$

where α_s is the running of the spectral index, β_s is the running of the running, and $k_\star = 0.05$ Mpc^{-1}.

The Planck temperature and polarization data analysis presented in Ref. [2], while providing a small indication for a *positive* running different from zero ($\alpha_s = 0.009 \pm 0.010$ at 68% C.L.), suggests also the presence of a running of the running at the level of two standard deviations ($\beta_s = 0.025 \pm 0.013$ at 68% C.L.). The inclusion of a running of the running improves the fit to the Planck temperature and polarization data by $\Delta\chi^2 \sim 5$ with respect to the ΛCDM model. Therefore, we do not expect that such an anomaly is due to the increased parameter volume and could be a hint of possible new physics beyond the standard model. A discussion of the impact of this anomaly on inflationary models has been presented in Refs. [11,12].

Given this result, it is timely to discuss the possible correlations between these three anomalies, β_s, A_L, and Ω_k and see, for example, if one of them vanishes if a second one is considered at the same time in the analysis. Moreover (related to the above points), it is necessary to investigate in more detail how the inclusion of β_s helps give a better fit to the data and test if the indication for the running of the running survives when additional data sets such as BAO or lensing (CMB and shear) are considered. This is the goal of this paper.

We structure the discussion as follows. In the next section, we will describe the analysis method and the cosmological data sets used. In Sec. III, we present our results and discuss possible correlations between β_s, A_L, and Ω_k. We also investigate the possibility that a running of the running affects current and future measurements of CMB spectral distortions, comparing our results with those of Ref. [13]. Finally, in Sec. VI, we derive our conclusions.

[1]E.g., we expect a running of the tilt n_s of order $(1 - n_s)^2$ in slow-roll inflation.

II. METHOD

We perform a Monte Carlo Markov chain (MCMC) analysis of the most recent cosmological data sets using the publicly available code `cosmomc` [14,15]. We consider the six parameters of the standard ΛCDM model, i.e., the baryon $\omega_b \equiv \Omega_b h^2$ and cold dark matter $\omega_c \equiv \Omega_c h^2$ energy densities, the angular size of the horizon at the last scattering surface θ_{MC}, the optical depth τ, the amplitude of primordial scalar perturbations $\log(10^{10} A_s)$, and the scalar spectral index n_s. We extend this scenario by including the running of the scalar spectral index α_s and the running of the running β_s. We fix the pivot scale at $k_\star = 0.05$ Mpc^{-1}. This is our baseline cosmological model, that we will call "base" in the following. Moreover, as discussed in the Introduction, we also consider separate variation in the lensing amplitude A_L, in the curvature density Ω_k, and in the sum of neutrino masses $\sum m_\nu$.

The main data set we consider, to which we refer as "Planck," is based on CMB temperature and polarization anisotropies. We analyze the temperature and polarization Planck likelihood [16]; more precisely, we make use of the *TT*, *TE*, *EE* high-ℓ likelihood together with the *TEB* pixel-based low-ℓ likelihood. The additional data sets we consider are the following:

(i) Planck measurements of the lensing potential power spectrum $C_\ell^{\phi\phi}$ [17];
(ii) weak gravitational lensing data of the CFHTLenS survey [18,19], taking only wave numbers $k \leq 1.5h$ Mpc^{-1} [1,20];
(iii) BAO: the surveys included are 6dFGS [21], SDSS-MGS [22], BOSS LOWZ [23], and CMASS-DR11 [23]. This data set will help to break geometrical degeneracies when we leave Ω_k free to vary.

III. RESULTS

In Table I, we present the constraints on n_s, α_s, and β_s from the Planck 2015 temperature and polarization data and in combination with BAO, cosmic shear, and CMB lensing. As we can see, the Planck-alone data set provides an indication for $\beta_s > 0$ at more than two standard deviations with $\beta_s = 0.027 \pm 0.013$ at 68% C.L.

It is interesting to investigate the impact of the inclusion of α_s and β_s on the remaining six parameters of the ΛCDM model. Comparing our results with those reported in Table 3 of Ref. [2], we see that there are no major shifts on the parameters. The largest shifts are present for the scalar spectral index n_s, that is ∼0.9 standard deviations *lower* when β_s is included, and for the reionization optical depth τ, that is ∼0.9 standard deviations *higher* with respect to the standard ΛCDM scenario. A similar shift is also present for the value of the root-mean-square density fluctuations on scales of $8h$ Mpc^{-1} (the σ_8 derived parameter), which is higher by about one standard deviation when β_s is considered. In Fig. 1, we plot the probability contour at

TABLE I. 68% C.L. bounds on $\Omega_b h^2$, $\Omega_c h^2$, $100\theta_{MC}$, τ, H_0, $\log(10^{10}A_s)$, n_s, α_s, β_s, for the listed data sets: the model is $\Lambda\mathrm{CDM} + \alpha_s + \beta_s$, $k_\star = 0.05$ Mpc^{-1}.

Base	Planck	+lensing	+WL	+BAO
$\Omega_b h^2$	0.02216 ± 0.00017	0.02215 ± 0.00017	0.02221 ± 0.00017	0.02224 ± 0.00015
$\Omega_c h^2$	0.1207 ± 0.0015	0.1199 ± 0.0015	0.1197 ± 0.0014	0.1196 ± 0.0011
$100\theta_{MC}$	1.0407 ± 0.00032	1.0408 ± 0.00032	1.04078 ± 0.00032	$1.04082^{+0.00029}_{-0.0003}$
τ	0.091 ± 0.019	0.064 ± 0.014	0.086 ± 0.019	0.096 ± 0.018
H_0	66.88 ± 0.68	67.16 ± 0.67	$67.29^{+0.66}_{-0.65}$	$67.36^{+0.49}_{-0.48}$
$\log(10^{10}A_s)$	3.118 ± 0.037	3.061 ± 0.026	$3.104^{+0.038}_{-0.037}$	3.125 ± 0.036
n_s	$0.9582^{+0.0055}_{-0.0054}$	0.9607 ± 0.0054	0.9608 ± 0.0055	$0.9613^{+0.0046}_{-0.0047}$
α_s	0.011 ± 0.01	0.012 ± 0.01	0.012 ± 0.01	0.01 ± 0.01
β_s	0.027 ± 0.013	0.022 ± 0.013	0.026 ± 0.013	0.025 ± 0.013

68% C.L. and 95% C.L. for the several combinations of data sets in the $\beta_s - \sigma_8$ and $\beta_s - \tau$ planes, respectively. Clearly, a new determination of τ from future large-scale polarization data as those expected from the Planck HFI experiment could have an impact on the value of β_s. On the other hand, this one sigma shift in τ with respect to ΛCDM shows that a large-scale measurement of CMB polarization does not fully provide a direct determination of τ but that some model dependence is present.

Moreover, as expected, there is a strong correlation between α_s and β_s. Because of this correlation, the running α_s is constrained to be positive, with $\alpha_s > 0$ at more than 68% C.L. when β_s is considered. This is a $\sim$1.3 standard deviations shift on α_s if we compare this result with the value obtained using the same data set but fixing $\beta_s = 0$ in Table 5 of Ref. [2]. In Fig. 2, we plot the two-dimensional likelihood constraints in the $n_s - \beta_s$ and $\alpha_s - \beta_s$ planes. As we can see, a correlation between the parameters is clearly present. However, when α_s and possibly higher derivatives of the scalar tilt are left free to vary, the constraints will depend on the choice of the pivot scale $k_\star$ [24]. We have therefore considered two additional values of $k_\star$, i.e., $k_\star = 0.01$ Mpc^{-1} and $k_\star = 0.002$ Mpc^{-1}; the resulting plots are shown in Sec. A 1 (where we also present a simple argument to explain the stability of σ_{β_s} under the change of $k_\star$), while Table II shows the 68% C.L. constraints on n_s, α_s, and β_s (base model, Planck TT, TE, EE + lowP data set).[2] From Table II, we see that, while the 1σ indication for $\alpha_s > 0$ disappears if we change $k_\star$ (becoming a $\sim 2\sigma$ evidence for negative running), β_s remains larger than zero at $\sim 2\sigma$.[3] We therefore conclude that the preference for blue β_s is stable under the variation of $k_\star$; by studying the improvement in χ^2 with respect to the ΛCDM and $\Lambda\mathrm{CDM} + \alpha_s$ models, we can understand what its origin is.

The Planck likelihood consists essentially of three terms: a low-ℓ ($\ell = 2$–29) TEB likelihood based on the Planck LFI 70 GHz channel full mission data set, a high-ℓ likelihood based on Planck HFI 100, 143, and 217 GHz channels half-mission data set, and, finally, an additional χ^2 term that comes from the external priors assumed on foregrounds (see Ref. [16]). By looking at the mean χ^2_{eff} values from these three terms, we can better understand from where (low ℓ, high ℓ, foregrounds) the indication for β_s is coming. Comparing with the χ^2 values obtained under standard ΛCDM with $\alpha_s = 0$ and $\beta_s = 0$, we have found that, while the high-ℓ likelihood remains unchanged, there is an improvement in the low-ℓ likelihood of $\Delta\chi^2_{\mathrm{eff}} \sim 2.5$ and in the foregrounds term with $\Delta\chi^2_{\mathrm{eff}} \sim 1$. The inclusion of β_s provides therefore a better fit to the low-ℓ part of the CMB spectrum and to the foregrounds prior. While the better fit to the low-ℓ part of the CMB spectrum can be easily explained by the low quadrupole TT anomaly and by the dip at $\ell \sim 20$–30, the change due to foregrounds is somewhat unexpected since, in general, foregrounds do not correlate with cosmological parameters. We have found a significant correlation between β_s and the point source amplitude at 143 GHz, A^{PS}_{143}. The posterior of A^{PS}_{143} shifts indeed by a half-sigma toward lower values with respect to the standard ΛCDM case (see Fig. 3) from $A^{\mathrm{PS}}_{143} = 43 \pm 8$ to $A^{\mathrm{PS}}_{143} = 39 \pm 8$ at 68% C.L. This shift could also explain the small difference between the constraints reported here and those reported in Ref. [2], that uses the Pliklite likelihood code where foregrounds are marginalized at their ΛCDM values.

Before proceeding, we stress that, using a likelihood ratio test [25], it is easy to see that, for a $\Delta\chi^2_{\mathrm{eff}} \sim 3.5$ (as the one we find here), there still is a $\sim$17% probability that the ΛCDM model is the correct one.[4] Given the Planck TT, TE, EE + lowP data set, this is the significance with which the $\Lambda\mathrm{CDM} + \alpha_s + \beta_s$ model is preferred over the ΛCDM one.

[2] A study of the impact of $k_\star$ when also A_L, $\sum m_\nu$, and Ω_K are varied is left to future work.

[3] We also note a $\sim 1\sigma$ indication of blue tilt when $k_\star$ is 0.002 Mpc^{-1}.

[4] Using the fact that $2\log(\mathcal{L}_1/\mathcal{L}_2)$ is distributed as a χ^2 with d.o.f. $=$ d.o.f.$_1$ $-$ d.o.f.$_2$.

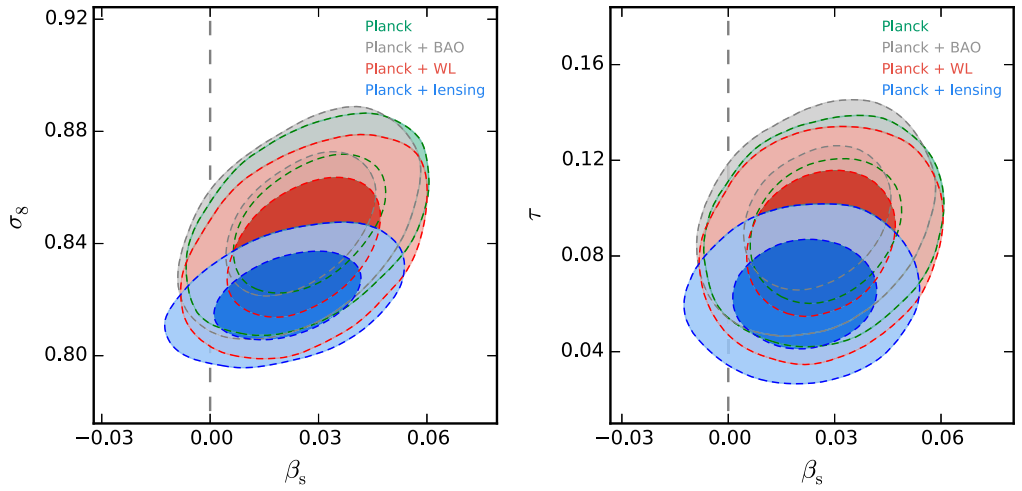

FIG. 1. Constraints at 68% C.L. and 95% C.L. in the $\beta_s - \sigma_8$ plane (left panel) and in the $\beta_s - \tau$ plane (right panel).

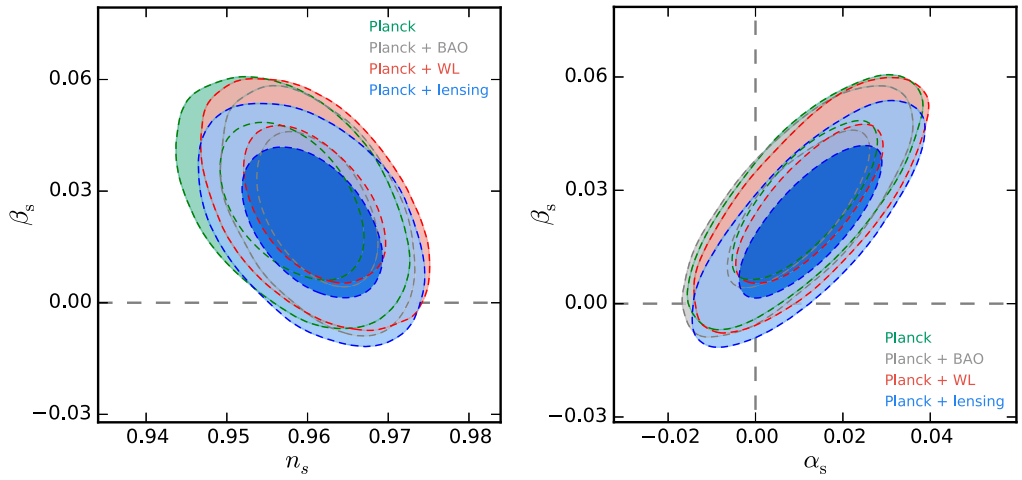

FIG. 2. Likelihood constraints in the $n_s - \beta_s$ (left panel) and $\alpha_s - \beta_s$ (right panel) planes for different combinations of data sets, as discussed in the text.

Going back to Table I, we can see that the indication for $\beta_s > 0$ is slightly weakened but still present also when external data sets are considered. Adding CMB lensing gives $\beta_s = 0.022 \pm 0.013$, i.e., reducing the tension to about 1.7 standard deviations, while the inclusion of weak lensing and BAO data does not lead to an appreciable decrease in the statistical significance of α_s and β_s.

In Table III, we report similar constraints but include also variations in the neutrino mass absolute scale $\sum m_\nu$. The constraints obtained from the Planck 2015 data release on the neutrino masses are indeed very strong, especially when combined with BAO data, ruling out the possibility of a direct detection from current and future beta and double beta decay experiments (see, e.g., Ref. [26]). Since Planck data show a preference for $\beta_s > 0$, it is clearly interesting to investigate if the inclusion of running has some impact on the cosmological constraints on $\sum m_\nu$. Comparing the results of Table III with those in Ref. [2], which were obtained assuming $\alpha_s = \beta_s = 0$, we see that the constraints on $\sum m_\nu$ are only slightly weakened, moving from $\sum m_\nu < 0.490$ eV to $\sum m_\nu < 0.530$ eV at 95% C.L. for the Planck data set alone and from $\sum m_\nu < 0.590$ eV to $\sum m_\nu < 0.644$ eV at 95% C.L. when also lensing is considered. The constraints on $\sum m_\nu$ including the weak

TABLE II. 68% C.L. constraints on n_s, α_s, β_s, for the listed pivot scales: the model is $\Lambda\mathrm{CDM} + \alpha_s + \beta_s$, and the data set is Planck (TT, TE, EE + lowP).

Base	$k_\star = 0.01$ Mpc^{-1}	$k_\star = 0.002$ Mpc^{-1}
n_s	$0.9758^{+0.0117}_{-0.0116}$	$1.0632^{+0.0466}_{-0.0459}$
α_s	-0.032 ± 0.015	-0.076 ± 0.035
β_s	0.027 ± 0.013	0.027 ± 0.013

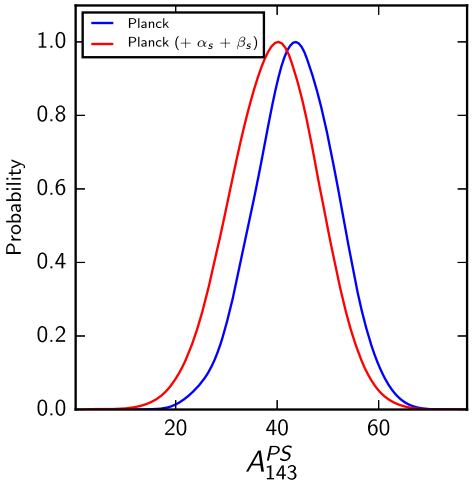

FIG. 3. Shift in the amplitude of unresolved foreground point sources at 143 GHz between the ΛCDM case and the case when variation in α_s and β_s is considered. The data set used is the Planck temperature and polarization angular spectra.

lensing (WL) and BAO data sets are essentially unaffected by β_s. We can therefore conclude that there is no significant correlation between β_s and $\sum m_\nu$.

In Fig. 4, we plot the posterior distributions for $\sum m_\nu$, while in Fig. 5, we plot the probability contour at 68% C.L. and 95% C.L. for the several combinations of data sets in the $\beta_s - \sum m_\nu$ plane.

In Table IV, we report the constraints from the same data sets but with also having left the lensing amplitude A_L free to vary. As discussed in the Introduction, Planck data are also suggesting a value for $A_L > 1$, and it is therefore interesting to check if there is a correlation with β_s. As we can see, there is a correlation between the two parameters, but it is not extremely significant. Even with a lower statistical significance, at about ∼1.2–1.5 standard deviations for A_L and β_s, respectively (that could be also explained by the increased volume of parameter space), data seem to suggest the presence of *both* anomalies. When the CMB lensing data are included, A_L goes back to its standard value, while the indication for β_s increases. When the WL shear data are included, the A_L anomaly is present, while the indication for β_s is weakened.

We also consider variation in the curvature of the universe, and we report the constraints in Table V. As we can see, also in this case, we have a correlation between β_s and Ω_k, but it is not significant enough to completely cancel any indication for these anomalies from Planck data. Indeed, when Ω_k is considered, we have still a preference for $\Omega_k < 0$ and $\beta_s > 0$ at more than one standard deviation. More interestingly, when external data sets are included, the indication for a positive curvature simply vanishes, while we get $\beta_s > 0$ slightly below 95% C.L.

In Fig. 6, we show the constraints at 68% C.L. and 95% C.L. in the $\beta_s - A_L$ plane (left panel) and in the $\beta_s - \Omega_k$ plane (right panel).

We conclude this section by looking at what the improvements (or nonimprovements) in χ^2 over our base model $\Lambda\mathrm{CDM} + \alpha_s + \beta_s$ are when additional parameters (A_L, $\sum m_\nu$ and Ω_K) are considered; the tables (Tables VII, VIII, IX, and X) containing all the $\Delta\chi^2$ (which we define by $\chi^2_{\rm base} - \chi^2_{\rm base+ext}$) are collected in Sec. A 2. When considering the $+A_L$ extension, we see that an improvement $\Delta\chi^2 \sim 1.5$ ($\Delta\chi^2 \sim 6$) is obtained for the Planck TT, TE, EE + lowP + BAO data set (Planck TT, TE, EE + lowP + WL data set), while the addition of CMB lensing data to Planck temperature and polarization data leads to $\Delta\chi^2 \sim -1.5$, mainly driven by a worse fit to the foregrounds. When $\sum m_\nu$ or Ω_K are left free to vary, we see that the fit to the data is in general worse; only when adding Ω_K to the Planck TT, TE, EE + lowP + WL data set do we get a $\Delta\chi^2 \sim 2$ improvement.

IV. PRESENT AND FUTURE CONSTRAINTS FROM μ-DISTORTIONS

CMB μ-type spectral distortions [28,29] from the dissipation of acoustic waves at redshifts between

TABLE III. 68% C.L. bounds and 95% C.L. upper limits on $\Omega_b h^2$, $\Omega_c h^2$, $100\theta_{\rm MC}$, τ, $\sum m_\nu$, H_0, $\log(10^{10}A_s)$, n_s, α_s, β_s, for the listed data sets: the model is $\Lambda\mathrm{CDM} + \alpha_s + \beta_s + \sum m_\nu$, $k_\star = 0.05$ Mpc^{-1}.

Base + $\sum m_\nu$	Planck	+ lensing	+ WL	+ BAO
$\Omega_b h^2$	0.02213 ± 0.00018	0.02207 ± 0.00019	0.02219 ± 0.00018	0.02224 ± 0.00015
$\Omega_c h^2$	0.1208 ± 0.0016	0.1206 ± 0.0016	0.1199 ± 0.0015	0.1196 ± 0.0011
$100\theta_{\rm MC}$	$1.04062^{+0.00033}_{-0.00034}$	1.0406 ± 0.00035	1.04072 ± 0.00033	1.04082 ± 0.0003
τ	$0.095^{+0.019}_{-0.02}$	0.08 ± 0.019	0.088 ± 0.02	$0.095^{+0.02}_{-0.019}$
$(\sum m_\nu)$/eV	< 0.53	< 0.644	< 0.437	< 0.159
H_0	$65.76^{+2.12}_{-0.99}$	$64.76^{+2.49}_{-1.7}$	$66.46^{+1.76}_{-0.91}$	67.38 ± 0.56
$\log(10^{10}A_s)$	$3.127^{+0.038}_{-0.039}$	$3.093^{+0.037}_{-0.036}$	3.109 ± 0.038	$3.124^{+0.037}_{-0.038}$
n_s	$0.9576^{+0.0056}_{-0.0057}$	0.9583 ± 0.0057	$0.9601^{+0.0055}_{-0.0054}$	$0.9612^{+0.0047}_{-0.0048}$
α_s	0.011 ± 0.01	0.011 ± 0.01	0.012 ± 0.01	$0.01^{+0.01}_{-0.011}$
β_s	0.028 ± 0.013	0.023 ± 0.013	0.026 ± 0.013	0.025 ± 0.013

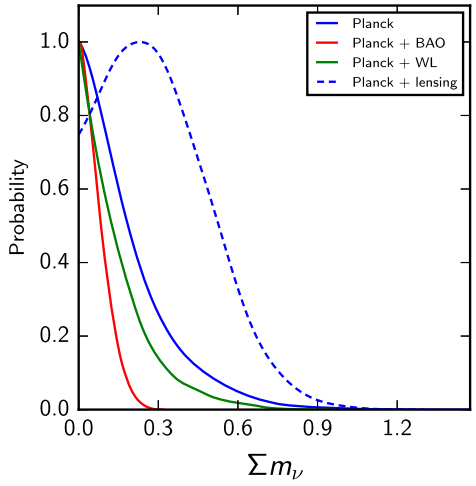

FIG. 4. One-dimensional posterior distributions for the sum of neutrino masses $\sum m_\nu$, for the indicated data sets. The model considered is $\Lambda\mathrm{CDM} + \alpha_s + \beta_s + \sum m_\nu$.

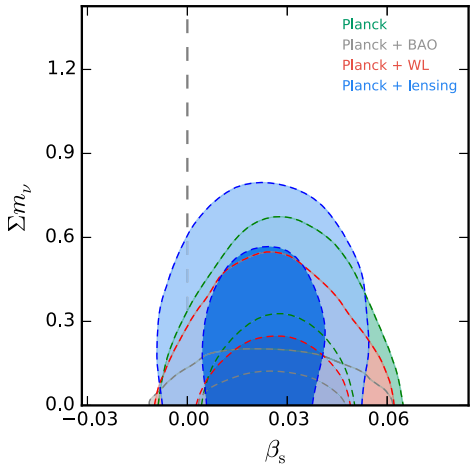

FIG. 5. Two-dimensional posteriors in the $\beta_s - \sum m_\nu$ plane, for the indicated data sets. We see that there is no correlation between $\sum m_\nu$ and β_s.

$z = 2 \times 10^6 \equiv z_{\mathrm{dC}}$ and $z = 5 \times 10^4 \equiv z_{\mu-y}$ offer a window on the primordial power spectrum at very small scales, ranging from 50 to 10^4 Mpc^{-1} (for most recent works on this topic, see Refs. [30–36] and references therein). The impact of a PIXIE-like mission on the constraints on the running α_s was recently analyzed in Ref. [35], while Refs. [32,36] also investigated the variety of signals (and corresponding forecasts) that are expected in the ΛCDM model (not limited to a μ-type distortion).

In this section, we briefly investigate the constraining power of μ distortions on β_s, given the Planck constraints on α_s and β_s of Sec. III. We compute the contribution to the μ monopole from Silk damping of acoustic waves in the photon-baryon plasma [37–41], using the expression for the distortion visibility function presented in Ref. [32].[5] To understand the relationship between the μ amplitude and the parameters of the primordial power spectrum, one can compute the (integrated) fractional energy that is dissipated by the acoustic waves δ_γ between $z = 2 \times 10^6$ and $z = 5 \times 10^4$; this energy feeds back into the background and generates μ distortions according to (see also Refs. [42,43])

$$\mu(\boldsymbol{x}) \approx \frac{1.4}{4} \langle \delta_\gamma^2(z, \boldsymbol{x}) \rangle_p \Big|_{z_{\mu-y}}^{z_{\mathrm{dC}}}, \tag{2}$$

where $\langle \ldots \rangle_p$ indicates the average over a period of oscillation and ζ is the primordial curvature perturbation. The diffusion damping length appearing in the above formula is given by [37–39]

$$k_{\mathrm{D}}(z) = \sqrt{\int_z^{+\infty} \mathrm{d}z \frac{1+z}{H n_e \sigma_T} \left[\frac{R^2 + \frac{16}{15}(1+R)}{6(1+R)^2} \right]}. \tag{3}$$

The observed μ-distortion monopole is basically the ensemble average of $\mu(\boldsymbol{x})$ at $z = 5 \times 10^4$; by averaging Eq. (2), then, one sees that it is equal to the log integral of the primordial power spectrum multiplied by a window function,

$$W_\mu(k) = 2.3 e^{-2k^2/k_D^2} \Big|_{z_{\mu-y}}^{z_{\mathrm{dC}}}, \tag{4}$$

which localizes the integral between 50 to 10^4 Mpc^{-1}.

Table VI shows how, already with the current limit on the μ-distortion amplitude from the FIRAS instrument on the COBE satellite, namely, $\mu = (1 \pm 4) \times 10^{-5}$ at 68% C.L. [27], we can get a 28% increase in the 95% C.L. upper limits on α_s and a 33% increase in those on β_s (we also stress that, in the case of β_s fixed to zero, including FIRAS does not result in any improvement on the bounds for α_s). In Fig. 7, we also report a forecast for PIXIE, the expected error on μ of which is 10^{-8} [44].[6] Besides, we see the following:

[5]This is related to the method called "Method II" in Ref. [36], the difference being that the visibility function $J_{\mathrm{bb}}(z)$ used: $J_{\mathrm{bb}}(z)$ is approximated to $\exp(-(z/z_{\mathrm{dC}})^{5/2})$ in Method II of Ref. [36], while Ref. [32] derives a fitting formula to take into account the dependence of $J_{\mathrm{bb}}(z)$ on cosmological parameters. At the large values of α_s and β_s allowed by Planck, we do not expect this difference to be very relevant for our final result.

[6]In Ref. [45], it was shown that, when also r distortions are considered, the expected error should be larger (about $\sigma_\mu = 1.4 \times 10^{-8}$); however, at the large values of α_s and β_s allowed by Planck, the forecasts of Table VI are not significantly affected. r distortions are the residual distortions that encode the information on the transition between the μ era (when distortions are of the μ type) and the y era (when the CMB is not in kinetic equilibrium and energy injections result in distortions of the y type). We refer to Refs. [46,47] for a study of these residual distortions and to Refs. [32,45] for a study of their constraining power on cosmological parameters.

TABLE IV. 68% C.L. bounds and 95% C.L. upper limits on $\Omega_b h^2$, $\Omega_c h^2$, $100\theta_{MC}$, τ, A_L, H_0, $\log(10^{10}A_s)$, n_s, α_s, β_s, for the listed data sets: the model is $\Lambda\mathrm{CDM} + \alpha_s + \beta_s + A_L$, $k_\star = 0.05$ Mpc^{-1}.

Base + A_L	Planck	+lensing	+WL	+BAO
$\Omega_b h^2$	0.02227 ± 0.00019	0.02214 ± 0.00018	0.02235 ± 0.00019	0.02232 ± 0.00016
$\Omega_c h^2$	0.1196 ± 0.0017	0.1202 ± 0.0017	0.1185 ± 0.0016	0.119 ± 0.0011
$100\theta_{MC}$	1.04081 ± 0.00033	1.04076 ± 0.00033	1.04093 ± 0.00033	1.04089 ± 0.0003
τ	0.07 ± 0.025	0.07 ± 0.025	< 0.095	$0.07^{+0.024}_{-0.026}$
A_L	$1.106^{+0.079}_{-0.09}$	$0.984^{+0.058}_{-0.064}$	$1.157^{+0.077}_{-0.086}$	$1.118^{+0.075}_{-0.084}$
H_0	67.38 ± 0.77	$67.04^{+0.75}_{-0.76}$	67.88 ± 0.73	$67.64^{+0.52}_{-0.53}$
$\log(10^{10}A_s)$	$3.073^{+0.05}_{-0.051}$	$3.074^{+0.05}_{-0.051}$	$3.044^{+0.044}_{-0.051}$	3.072 ± 0.049
n_s	0.9621 ± 0.0062	0.9597 ± 0.0061	$0.9652^{+0.0059}_{-0.006}$	0.9637 ± 0.0049
α_s	0.01 ± 0.01	0.012 ± 0.01	0.01 ± 0.01	0.009 ± 0.01
β_s	0.021 ± 0.014	0.024 ± 0.014	0.018 ± 0.013	0.019 ± 0.013

TABLE V. 68% C.L. bounds on $\Omega_b h^2$, $\Omega_c h^2$, $100\theta_{MC}$, τ, Ω_K, H_0, σ_8, $\log(10^{10}A_s)$, n_s, α_s, β_s, for the listed data sets: the model is $\Lambda\mathrm{CDM} + \alpha_s + \beta_s + \Omega_K$, $k_\star = 0.05$ Mpc^{-1}.

Base + Ω_K	Planck	+lensing	+WL	+BAO
$\Omega_b h^2$	0.0223 ± 0.00019	0.02213 ± 0.00018	0.02214 ± 0.00019	0.02218 ± 0.00018
$\Omega_c h^2$	$0.1192^{+0.0017}_{-0.0018}$	0.1204 ± 0.0017	0.1206 ± 0.0017	0.1205 ± 0.0016
$100\theta_{MC}$	1.04086 ± 0.00034	1.04074 ± 0.00033	$1.04068^{+0.00035}_{-0.00034}$	$1.04072^{+0.00033}_{-0.00034}$
τ	$0.062^{+0.024}_{-0.028}$	0.076 ± 0.026	$0.099^{+0.023}_{-0.024}$	0.094 ± 0.018
Ω_K	$-0.0302^{+0.025}_{-0.0173}$	$0.0045^{+0.0096}_{-0.0076}$	$0.0082^{+0.0091}_{-0.0071}$	0.0015 ± 0.0021
H_0	$57.75^{+4.81}_{-6.34}$	$69.71^{+4.11}_{-4.62}$	$71.7^{+3.91}_{-5.02}$	$67.72^{+0.71}_{-0.72}$
σ_8	$0.799^{+0.033}_{-0.036}$	0.837 ± 0.029	$0.86^{+0.026}_{-0.027}$	0.85 ± 0.016
$\log(10^{10}A_s)$	$3.057^{+0.048}_{-0.058}$	3.087 ± 0.052	$3.133^{+0.047}_{-0.049}$	$3.124^{+0.036}_{-0.037}$
n_s	$0.9642^{+0.0064}_{-0.0065}$	$0.9589^{+0.0064}_{-0.0063}$	0.9574 ± 0.0063	0.9587 ± 0.0057
α_s	$0.008^{+0.01}_{-0.011}$	0.013 ± 0.01	0.014 ± 0.011	0.011 ± 0.01
β_s	0.013 ± 0.014	$0.027^{+0.015}_{-0.017}$	$0.035^{+0.015}_{-0.017}$	0.027 ± 0.014

(i) For the best-fit values of cosmological parameters in the $\Lambda\mathrm{CDM} + \alpha_s + \beta_s$ model, which leads to $\mu = 1.09 \times 10^{-6}$, PIXIE will be able to detect spectral distortions from Silk damping at extremely high significance (Fig. 7). Besides, we see that a statistically significant detection of β_s is expected, along with a sizable shrinking of the available parameter space (Fig. 7). As we discuss later, any

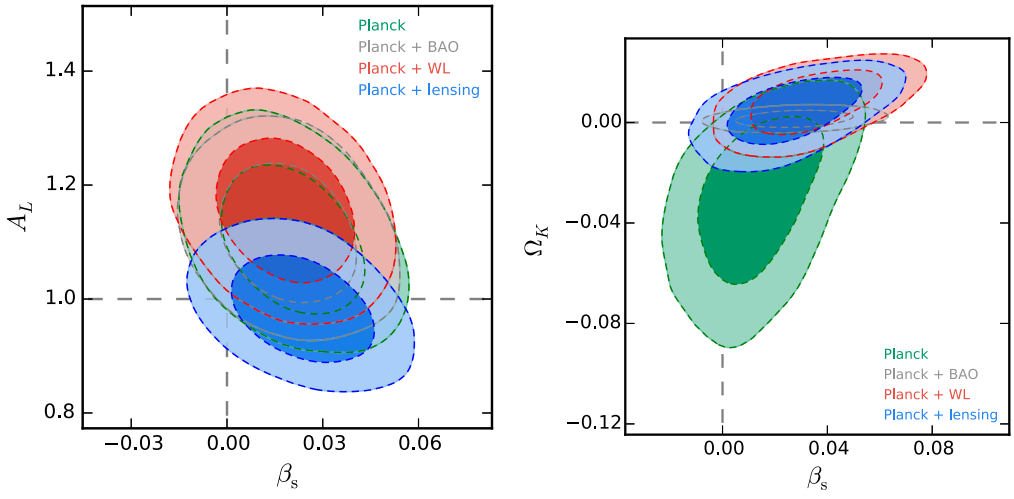

FIG. 6. Constraints at 68% C.L. and 95% C.L. in the $\beta_s - A_L$ plane (left panel) and in the $\beta_s - \Omega_k$ plane (right panel).

TABLE VI. 95% C.L. bounds on α_s and β_s from the Planck (TT, TE, $EE+\text{lowP}$), Planck + FIRAS, and Planck + PIXIE data sets, for the $\Lambda\text{CDM}+\alpha_s+\beta_s$ (i.e., base) model. The results have been obtained by postprocessing with a Gaussian likelihood the Markov chains considering $\mu=(1.0\pm4.0)\times10^{-5}$ [27] for FIRAS and $\mu=(1.57\pm1.00)\times10^{-8}$ for PIXIE. See the main text for a discussion of the bounds on the μ amplitude.

Base	α_s	β_s	μ
Planck	0.011 ± 0.021	0.027 ± 0.027	/
+FIRAS	$0.006^{+0.017}_{-0.018}$	$0.020^{+0.016}_{-0.019}$	$(0.77^{+3.10}_{-0.77})\times10^{-6}$
+PIXIE	$-0.007^{+0.012}_{-0.013}$	$0.001^{+0.008}_{-0.009}$	$(1.59^{+1.75}_{-1.52})\times10^{-8}$

TABLE VII. χ^2 comparison between the base $\Lambda\text{CDM}+\alpha_s+\beta_s$ model and the other extensions considered in the main text, for the Planck TT, TE, $EE+\text{lowP}$ data set. The last line contains the overall $\Delta\chi^2$ for all the likelihoods included in the analysis.

	vs $+A_L$	vs $+\sum m_\nu$	vs $+\Omega_K$
$\Delta\chi^2_{\text{plik}}$	2.1	−1.8	2.4
$\Delta\chi^2_{\text{lowP}}$	−0.9	−0.6	−1.3
$\Delta\chi^2_{\text{prior}}$	−1.	0.1	−1.9
$\Delta\chi^2$	0.2	−2.3	−0.7

TABLE VIII. Same as Table VII but with the addition of CMB lensing data.

	vs $+A_L$	vs $+\sum m_\nu$	vs $+\Omega_K$
$\Delta\chi^2_{\text{plik}}$	1.9	−0.5	1.5
$\Delta\chi^2_{\text{lowP}}$	−0.5	0.1	0.0
$\Delta\chi^2_{\text{prior}}$	−3.8	−2.7	−0.1
$\Delta\chi^2_{\text{lensing}}$	0.9	1.5	−1.3
$\Delta\chi^2$	−1.6	−1.6	0.1

TABLE IX. Same as Table VII; the data set is Planck TT, TE, $EE+\text{lowP}+\text{WL}$.

	vs $+A_L$	vs $+\sum m_\nu$	vs $+\Omega_K$
$\Delta\chi^2_{\text{plik}}$	3.0	−4.3	−1.6
$\Delta\chi^2_{\text{lowP}}$	−0.3	0.8	−0.3
$\Delta\chi^2_{\text{prior}}$	0.8	2.9	0.1
$\Delta\chi^2_{\text{CFHTLenS}}$	2.3	−0.6	3.8
$\Delta\chi^2$	5.9	−1.3	2.0

TABLE X. $\Delta\chi^2$ for the Planck TT, TE, $EE+\text{lowP}+\text{BAO}$ data set.

	vs $+A_L$	vs $+\sum m_\nu$	vs $+\Omega_K$
$\Delta\chi^2_{\text{plik}}$	0.7	1.0	−2.7
$\Delta\chi^2_{\text{lowP}}$	−1.8	−1.2	−1.
$\Delta\chi^2_{\text{prior}}$	1.4	0.3	0.8
$\Delta\chi^2_{\text{6DF}}$	0.1	0.0	0.1
$\Delta\chi^2_{\text{MGS}}$	−0.8	0.0	−0.8
$\Delta\chi^2_{\text{DR11CMASS}}$	0.9	0.1	1.1
$\Delta\chi^2_{\text{DR11LOWZ}}$	1.1	0.1	1.1
$\Delta\chi^2$	1.5	0.3	−1.4

detection of such values of μ distortions will rule out single-field slow-roll inflation, if we assume that all the generated distortions are due to Silk damping and not to other mechanisms like, for example, decaying dark matter particles.[7]

(ii) For a fiducial value of μ corresponding to the ΛCDM best fit, i.e., $\mu=1.57\times10^{-8}$ [35], we see that we get a 84% increase in the 95% C.L. upper limits on α_s and a 83% increase in those on β_s. More precisely, values of β_s larger than 0.02 will be excluded at $\sim5\sigma$.

We conclude this section with a comment on the validity of a Taylor expansion (in $\log k/k_\star$) of the power spectrum down to scales probed by spectral distortions. We can estimate the terms in the expansion of $n_s(k)$ by choosing $k=10^4\ \text{Mpc}^{-1}$, corresponding to k_D at $z=z_{dC}$: for values of β_s of order 0.06 (which are still allowed at 95% C.L., as shown in Fig. 7), the term $\frac{\beta_s}{6}(\log k/k_\star)^2$ in Eq. (1) becomes of order 1. For this reason, Table VI does not report the limits on μ coming from the current Planck constraints on the scale dependence of the spectrum. When existing limits on μ from FIRAS are instead added, an extrapolation of $\Delta^2_\zeta(k)$ at the scales probed by μ distortions starts to become meaningful, and when also PIXIE is included in our forecast around the ΛCDM prediction, the upper bounds on α_s and β_s are lowered enough that a perturbative expansion becomes viable, making our forecast valid.

V. LARGE β_s AND SLOW-ROLL INFLATION

In this section, we discuss briefly the implications that values of α_s and β_s of order 10^2 have for slow-roll inflation. We can compute the running of the slow-roll parameter ϵ in terms of n_s, α_s, and β_s by means of the simple slow-roll relations

[7]We did not investigate, in this work, whether it could be possible to have models of multifield inflation (or models where the slow-roll assumption is relaxed [48]) that can predict such values for the μ-distortion amplitude. We refer to Ref. [33] for an analysis of some multifield scenarios.

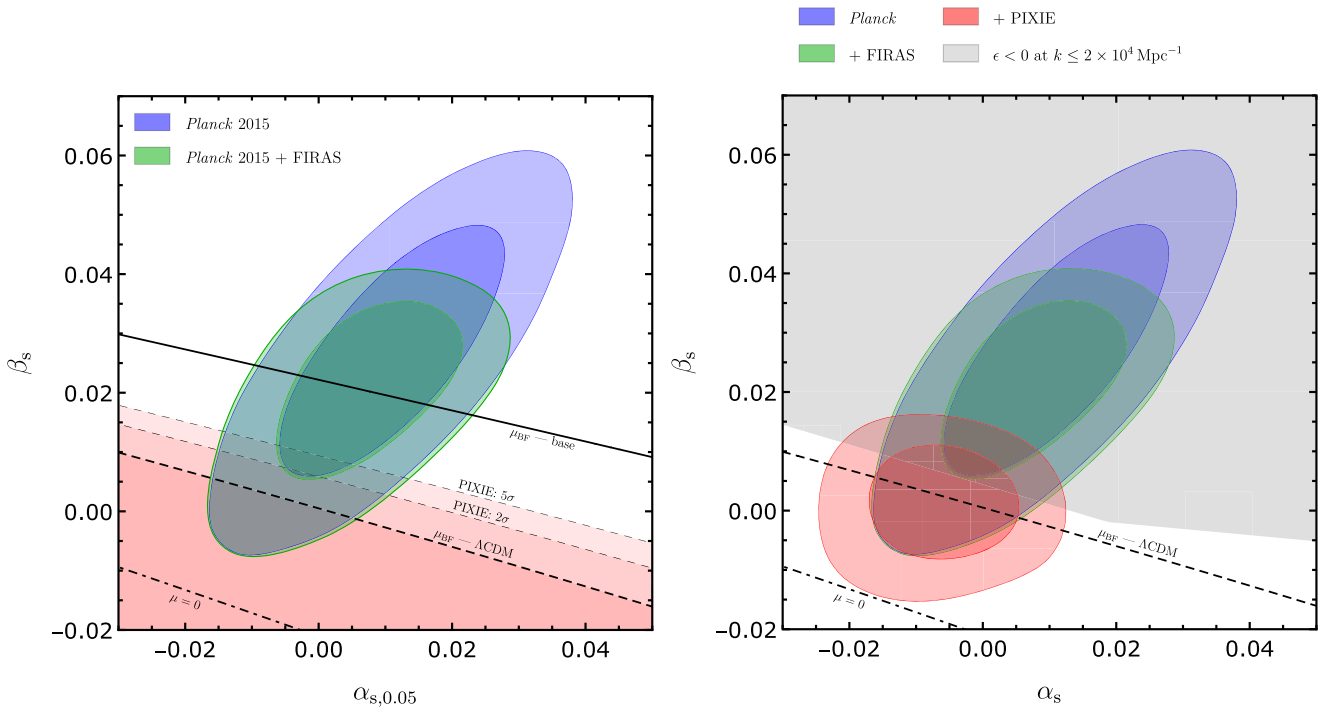

FIG. 7. Left panel: 68% C.L. and 95% C.L. contours in the $\alpha_{\rm s}$—$\beta_{\rm s}$ plane, for the Planck (blue) and Planck + FIRAS (green) data sets (base model). The red regions represent the 2σ and 5σ limits from PIXIE around the Planck best fit for the ΛCDM model, i.e., $\mu = 1.57 \times 10^{-8}$ [35]. Right panel: same as left panel, with the red contours representing the 68% C.L. and 95% C.L. limits from PIXIE, obtained by postprocessing the Markov chains with a Gaussian likelihood $\mu = (1.57 \pm 1.00) \times 10^{-8}$. The gray region represents the values of $\alpha_{\rm s}$ and $\beta_{\rm s}$ that lead to a slow-roll parameter $\epsilon(k)$, computed via the Taylor expansion of Eq. (6), less than zero before or at $k = 2 \times 10^4$ Mpc^{-1}.

$$N - N_\star = -\log\frac{k}{k_\star}, \tag{5a}$$

$$1 - n_{\rm s} = 2\epsilon - \frac{1}{\epsilon}\frac{{\rm d}\epsilon}{{\rm d}N}, \tag{5b}$$

where N is the number of e-foldings from the end of inflation, decreasing as time increases (i.e., $H{\rm d}t = -{\rm d}N$), and Eq. (5a) holds we if neglect the time derivative of the inflaton speed of sound $c_{\rm s}$. The running of ϵ up to third order in N is given, then, by

$$\epsilon(N) = \epsilon(N_\star) + \sum_{i=1}^{3}\frac{\epsilon^{(i)}}{i!}(N - N_\star)^i, \tag{6}$$

where the coefficients $\epsilon^{(i)}$ are given in Sec. A 3.

At scales around $k_\star$, $n_{\rm s}$ dominates so that ϵ is increasing and a red spectrum is obtained. However, in the presence of positive $\alpha_{\rm s}$ and $\beta_{\rm s}$, at small scales ϵ becomes smaller, until it becomes zero at $k \approx 39.7$ Mpc^{-1} for $\alpha_{\rm s} = 0.01$ and $\beta_{\rm s} = 0.02$ (taking $\epsilon_\star = 0.002$, i.e., the maximum value allowed by current bounds on r, when the inflaton speed of sound $c_{\rm s}$ is fixed to 1). If we impose that ϵ stays positive down to $k \approx 2 \times 10^4$ Mpc^{-1}, which is of the same order of magnitude of the maximum k probed by μ distortions (see Sec. IV), we can obtain a theoretical bound on $\alpha_{\rm s}$ and $\beta_{\rm s}$. We show this bound in Fig. 7; this plot tells us that a large part of the contours from Planck + FIRAS and Planck + PIXIE cannot be interpreted in the context of slow-roll inflation extrapolated to μ-distortion scales, because ϵ becomes negative before reaching $k \approx k_{\rm D}(z_{\rm dC})$.[8]

A similar discussion was presented in Ref. [13]; by means of a slow-roll reconstruction of the inflaton potential [50,51], it was shown that if $\beta_{\rm s}$ is controlled only by leading-order terms in the slow-roll expansion (see Sec. A 3) it is not possible to find a single-field inflation model that fits the posteriors from Planck.

These kind of bounds tell us that the Taylor expansion is not suitable for extrapolating the inflationary spectrum far away from the CMB window, in the presence of the values of $\alpha_{\rm s}$ and $\beta_{\rm s}$ that are currently allowed by Planck, since ϵ becomes zero already ~ 7 e-folds after the horizon exit of $k_\star$. To avoid this problem, one could consider a series expansion that takes into account the theoretical bounds on ϵ, i.e., $\epsilon(N = 0) = 1$ and $0 < \epsilon < 1$; the Taylor series does not respect these requirements, so it does *not* in general

[8]We point out that it is possible to obtain large positive $\alpha_{\rm s}$ and $\beta_{\rm s}$ in slow-roll inflation when modulations of the potential are considered [49]. However, we will not consider such models in this work.

represent a possible power spectrum from inflation, over the whole range of scales. Only when the values of the phenomenological parameters describing the scale dependence of the spectrum are small, the Taylor expansion can be a good approximation of a realistic power spectrum over a range of scales much larger than those probed by the CMB.

Another possibility is to consider bounds on the primordial power spectrum coming from observables that lie outside the CMB scales but that are still at small enough k that the Taylor series applies. These would be complementary to spectral distortions, which are basically sensitive only to scales around 740 Mpc^{-1} [31,45], opening the possibility of multiwavelength constraints on the scale dependence of the spectrum.

In this regard, observations of the Ly-α forest could be very powerful (the forest constrains wave numbers $k \approx 1h\ \mathrm{Mpc}^{-1}$),[9] In Ref. [54], an analysis of the one-dimensional Ly-α forest power spectrum measured in Ref. [55] was carried out, showing that it provides also small-scale constraints on the tilt n_s and the running α_s; more precisely, for a $\Lambda\mathrm{CDM} + \alpha_\mathrm{s} + \sum m_\nu$ model, a detection at approximately 3σ of α_s ($\alpha_\mathrm{s} = -0.00135^{+0.0046}_{-0.0050}$ at 68% C.L.) is obtained. It would be interesting to carry out this analysis including the running of the running, to see if the bounds on β_s are also lowered.

VI. CONCLUSIONS

In this paper, we have presented new constraints on the running of the running of the scalar spectral index β_s and discussed in more detail the 2σ indication for $\beta_\mathrm{s} > 0$ that comes from the analysis of CMB anisotropies data from the Planck satellite.

We have extended previous analyses by considering simultaneous variations in the lensing amplitude parameter A_L and the curvature of the universe Ω_k. We have found that, while a correlation does exist between these parameters, Planck data still hint for nonstandard values in the extended $\Lambda\mathrm{CDM} + \alpha_\mathrm{s} + \beta_\mathrm{s} + A_L$ and $\Lambda\mathrm{CDM} + \alpha_\mathrm{s} + \beta_\mathrm{s} + \Omega_k$ model, only partially suggesting a common origin for their anomalous signal related to the low CMB quadrupole. We have found that the Planck constraints on neutrino masses $\sum m_\nu$ are essentially stable under the inclusion of β_s.

We have shown how future measurements of CMB μ-type spectral distortions from the dissipation of acoustic waves, such as those expected by PIXIE, could severely constrain both the running and the running of the running. More precisely, we have found that an improvement on Planck bounds by a factor of $\sim 80\%$ is expected. Finally, we discussed the conditions under which the phenomenological expansion of the primordial power spectrum in Eq. (1) can be extended to scales much shorter that those probed by CMB anisotropies and can provide a good approximation to the predictions of inflationary models.

[9]Even if modeling the ionization state and thermodynamic properties of the intergalactic medium to convert flux measurements into a density power spectrum is very challenging (see Refs. [52] and [53] for a discussion).

ACKNOWLEDGMENTS

We would like to thank Jens Chluba and Takeshi Kobayashi for the careful reading of the manuscript and useful comments. We would also like to thank the referee for providing useful comments. G. C. and A. M. are supported by the Theoretical Astroparticle Physics research Grant No. 2012CPPYP7 under the program PRIN 2012 funded by MIUR and by TASP, INFN specific initiative. E. P. is supported by the Delta-ITP consortium, a program of the Netherlands organization for scientific research that is funded by the Dutch Ministry of Education, Culture and Science. This work has been done within the Labex ILP (Reference No. ANR-10-LABX-63) part of the Idex SUPER and received financial state aid managed by the Agence Nationale de la Recherche, as part of the program Investissements d'Avenir under Reference No. ANR-11-IDEX-0004-02. E. D. V. acknowledges the support of the European Research Council via Grant No. 267117 (DARK, P. I. Joseph Silk).

APPENDIX

1. Dependence on the choice of pivot scale

When including derivatives of the scalar spectral index as free parameters, one can expect that the constraints on them will depend on the choice of pivot scale $k_\star$ [24]; for example, for Planck, the pivot $k_\star = 0.05\ \mathrm{Mpc}^{-1}$ is chosen to decorrelate n_s and α_s. For this reason, we considered two additional values of $k_\star$ in the analysis of the base ($\Lambda\mathrm{CDM} + \alpha_\mathrm{s} + \beta_\mathrm{s}$) model with Planck ($TT$, TE, $EE+\mathrm{lowP}$) data: $k_\star = 0.01\ \mathrm{Mpc}^{-1}$ and $k_\star = 0.002\ \mathrm{Mpc}^{-1}$. We report the results in Figs. 8 and 9 and Table II; we see that at $k_\star = 0.01\ \mathrm{Mpc}^{-1}$ the tilt and β_s decorrelate, while the degeneracy between α_s and β_s goes from positive to negative. For $k_\star = 0.002\ \mathrm{Mpc}^{-1}$, instead, we see that α_s and β_s are still negatively correlated, while the degeneracy between n_s and β_s becomes positive. However, we see from Table II that, while changing the pivot cancels the 1σ indication for $\alpha_\mathrm{s} > 0$, the 2σ preference for $\beta_\mathrm{s} > 0$ remains in both cases.

We can understand why the marginalized error on β_s does not change if we change the pivot scale $k_\star$ with a simple Fisher analysis. For a log likelihood for $\boldsymbol{n} \equiv (n_\mathrm{s}, \alpha_\mathrm{s}, \beta_\mathrm{s})$ (marginalized over all parameters except n_s, α_s, β_s) given by

$$\mathcal{L}|_{k_\star^{(0)}} \propto (\boldsymbol{n} - \boldsymbol{n}_0)^T \cdot F_{k_\star^{(0)}} \cdot (\boldsymbol{n} - \boldsymbol{n}_0), \tag{A1}$$

with inverse covariance matrix $F_{k_\star^{(0)}}$, a change of pivot will result in

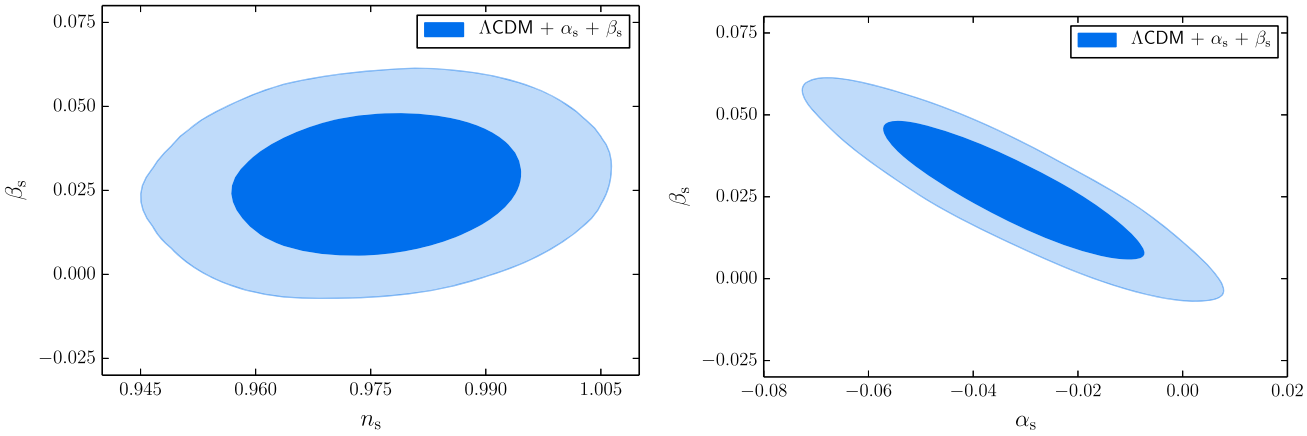

FIG. 8. Likelihood constraints in the $n_s - \beta_s$ (left panel) and $\alpha_s - \beta_s$ (right panel) planes for Planck (TT, TE, EE + lowP), at a pivot $k_\star = 0.01$ Mpc^{-1}.

$$\mathcal{L}|_{k_\star} \propto (M \cdot \boldsymbol{n} - \boldsymbol{n}_0)^T \cdot F_{k_\star^{(0)}} \cdot (M \cdot \boldsymbol{n} - \boldsymbol{n}_0), \quad \text{(A2)}$$

where M is given by the scale dependence of $\boldsymbol{n}$, i.e.,

$$\boldsymbol{n}_{k_\star} = M \cdot \boldsymbol{n}_{k_\star^{(0)}} = \begin{pmatrix} 1 & \log\frac{k_\star}{k_\star^{(0)}} & \frac{1}{2}\log^2\frac{k_\star}{k_\star^{(0)}} \\ 0 & 1 & \log\frac{k_\star}{k_\star^{(0)}} \\ 0 & 0 & 1 \end{pmatrix} \begin{pmatrix} n_s(k_\star^{(0)}) \\ \alpha_s(k_\star^{(0)}) \\ \beta_s(k_\star^{(0)}) \end{pmatrix}, \quad \text{(A3)}$$

and it is straightforward to verify that it has unit determinant. For a Gaussian likelihood, we can forget about $\boldsymbol{n}_0$ (we can just call $\boldsymbol{n}_0 = M \cdot \boldsymbol{m}_0$ and do a translation) so that all information will be coming from the transformed inverse covariance, i.e.,

$$F_{k_\star} = M^T \cdot F_{k_\star^{(0)}} \cdot M. \quad \text{(A4)}$$

Since M has unit determinant, the "figure of merit" f.o.m. $\propto 1/\det F_{k_\star}$ (which is basically 1/volume of a 68% C.L. ellipsoid) will not change if we change the pivot. What will indeed change are the marginalized and nonmarginalized 1σ errors on the parameters; however, it is straightforward to show with linear algebra that the marginalized error on the running of the running, which is given by

$$\sigma(\beta_s(k_\star)) = \sqrt{(F^{-1}_{k_\star})_{33}}, \quad \text{(A5)}$$

does not change under the transformation of Eq. (A3).

This simple picture does not explain why the mean values of n_s and α_s change. We ascribe this to the presence of the additional parameter A_s; under the transformation of Eq. (A3), it will not change linearly, so the Gaussian approximation will not hold. The data will still constrain A_s well enough so that $\sigma(A_s)$ will not contribute to the errors

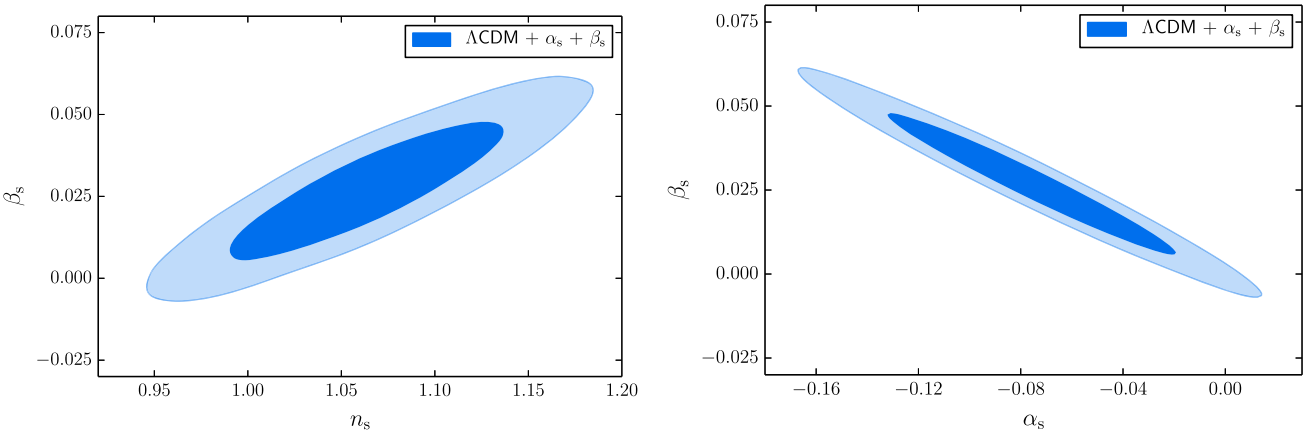

FIG. 9. Likelihood constraints in the $n_s - \beta_s$ (left panel) and $\alpha_s - \beta_s$ (right panel) planes for Planck (TT, TE, EE + lowP), at a pivot $k_\star = 0.002$ Mpc^{-1}.

on the parameters, but the position of the peak of the transformed likelihood will change.

2. $\Delta\chi^2$: Base model vs extensions

In this Appendix, we collect the full $\Delta\chi^2$ tables; we refer to Sec. III for a discussion of the various improvements and nonimprovements in χ^2 for the different choices of data sets and parameters that have been considered. In all the tables below, $\Delta\chi^2$ stands for $\chi^2_{\rm base}-\chi^2_{\rm base+ext}$, both obtained via MCMC sampling of the likelihood.

3. Derivation of slow-roll expansion for ϵ

Starting from Eq. (5b), differentiating it with respect to N, and then using Eq. (5a), one can find the coefficients $\epsilon^{(i)}$ of a Taylor expansion of $\epsilon(N)$ in terms of the parameters describing the scale dependence of the primordial spectrum $\Delta^2_\zeta(k)$. More precisely, one finds [calling $\epsilon_\star\equiv\epsilon(N_\star)$]

$$\epsilon^{(1)}=(n_{\rm s}-1)\epsilon_\star+2\epsilon_\star^2, \tag{A6a}$$

$$\epsilon^{(2)}=-\alpha_{\rm s}\epsilon_\star+4\epsilon_\star\epsilon^{(1)}+(n_{\rm s}-1)\epsilon^{(1)}, \tag{A6b}$$

$$\begin{aligned}\epsilon^{(3)}=&\,\beta_{\rm s}\epsilon_\star-2\alpha_{\rm s}\epsilon^{(1)}\\&+(n_{\rm s}-1)\{-\alpha_{\rm s}\epsilon_\star+4\epsilon_\star\epsilon^{(1)}+(n_{\rm s}-1)\epsilon^{(1)}\}\\&+4\{\epsilon_\star[-\alpha_{\rm s}\epsilon_\star+4\epsilon_\star\epsilon^{(1)}+(n_{\rm s}-1)\epsilon^{(1)}]+(\epsilon^{(1)})^2\}.\end{aligned} \tag{A6c}$$

By plugging in the values of $\alpha_{\rm s}$ and $\beta_{\rm s}$ allowed by Planck, one can extrapolate ϵ at scales different from $k_\star$. See Sec. V for a discussion.

[1] P. A. R. Ade *et al.* (Planck Collaboration), arXiv:1502.01589.
[2] P. A. R. Ade *et al.* (Planck Collaboration), arXiv:1502.02114.
[3] E. Calabrese, A. Slosar, A. Melchiorri, G. F. Smoot, and O. Zahn, Phys. Rev. D **77**, 123531 (2008).
[4] E. Di Valentino, A. Melchiorri, and J. Silk, Phys. Rev. D **93**, 023513 (2016).
[5] Z. Huang, Phys. Rev. D **93**, 043538 (2016).
[6] M. Gerbino, E. Di Valentino, and N. Said, Phys. Rev. D **88**, 063538 (2013).
[7] J. B. Muñoz, D. Grin, L. Dai, M. Kamionkowski, and E. D. Kovetz, Phys. Rev. D **93**, 043008 (2016).
[8] F. Couchot, S. Henrot-Versillé, O. Perdereau, S. Plaszczynski, B. R. d'Orfeuil, and M. Tristram, arXiv:1510.07600.
[9] G. E. Addison, Y. Huang, D. J. Watts, C. L. Bennett, M. Halpern, G. Hinshaw, and J. L. Weiland, Astrophys. J. **818**, 132 (2016).
[10] E. Di Valentino, A. Melchiorri, and J. Silk, Phys. Rev. D **92**, 121302 (2015).
[11] M. Escudero, H. Ramírez, L. Boubekeur, E. Giusarma, and O. Mena, J. Cosmol. Astropart. Phys. 02 (2016) 020.
[12] Q. G. Huang, K. Wang, and S. Wang, arXiv:1512.07769.
[13] B. A. Powell, arXiv:1209.2024.
[14] A. Lewis and S. Bridle, Phys. Rev. D **66**, 103511 (2002).
[15] A. Lewis, Phys. Rev. D **87**, 103529 (2013).
[16] N. Aghanim *et al.* (Planck Collaboration).
[17] P. A. R. Ade *et al.* (Planck Collaboration).
[18] C. Heymans *et al.*, Mon. Not. R. Astron. Soc. **427**, 146 (2012).
[19] T. Erben *et al.*, Mon. Not. R. Astron. Soc. **433**, 2545 (2013).
[20] T. D. Kitching *et al.* (CFHTLenS Collaboration), Mon. Not. R. Astron. Soc. **442**, 1326 (2014).
[21] F. Beutler, C. Blake, M. Colless, D. H. Jones, L. Staveley-Smith, L. Campbell, Q. Parker, W. Saunders, and F. Watson, Mon. Not. R. Astron. Soc. **416**, 3017 (2011).
[22] A. J. Ross, L. Samushia, C. Howlett, W. J. Percival, A. Burden, and M. Manera, Mon. Not. R. Astron. Soc. **449**, 835 (2015).
[23] L. Anderson *et al.* (BOSS Collaboration), Mon. Not. R. Astron. Soc. **441**, 24 (2014).
[24] M. Cortes, A. R. Liddle, and P. Mukherjee, Phys. Rev. D **75**, 083520 (2007).
[25] A. R. Liddle, Mon. Not. R. Astron. Soc. **351**, L49 (2004).
[26] M. Gerbino, M. Lattanzi, and A. Melchiorri, Phys. Rev. D **93**, 033001 (2016).
[27] D. J. Fixsen, E. S. Cheng, J. M. Gales, J. C. Mather, R. A. Shafer, and E. L. Wright, Astrophys. J. **473**, 576 (1996).
[28] Y. B. Zeldovich and R. A. Sunyaev, Astrophys. Space Sci. **4**, 301 (1969).
[29] R. A. Sunyaev and Y. B. Zeldovich, Astrophys. Space Sci. **7**, 20 (1970).
[30] J. B. Dent, D. A. Easson, and H. Tashiro, Phys. Rev. D **86**, 023514 (2012).
[31] J. Chluba, A. L. Erickcek, and I. Ben-Dayan, Astrophys. J. **758**, 76 (2012).
[32] R. Khatri and R. A. Sunyaev, J. Cosmol. Astropart. Phys. 06 (2013) 026.
[33] S. Clesse, B. Garbrecht, and Y. Zhu, J. Cosmol. Astropart. Phys. 10 (2014) 046.
[34] K. Enqvist, T. Sekiguchi, and T. Takahashi, J. Cosmol. Astropart. Phys. 04 (2016) 057.

[35] G. Cabass, A. Melchiorri, and E. Pajer, Phys. Rev. D **93**, 083515 (2016).
[36] J. Chluba, arXiv:1603.02496.
[37] J. Silk, Astrophys. J. **151**, 459 (1968).
[38] P. J. E. Peebles and J. T. Yu, Astrophys. J. **162**, 815 (1970).
[39] N. Kaiser, Mon. Not. R. Astron. Soc. **202**, 1169 (1983).
[40] W. Hu and J. Silk, Phys. Rev. D **48**, 485 (1993).
[41] J. Chluba, R. Khatri, and R. A. Sunyaev, Mon. Not. R. Astron. Soc. **425**, 1129 (2012).
[42] E. Pajer and M. Zaldarriaga, J. Cosmol. Astropart. Phys. 02 (2013) 036.
[43] E. Pajer and M. Zaldarriaga, Phys. Rev. Lett. **109**, 021302 (2012).
[44] A. Kogut *et al.*, J. Cosmol. Astropart. Phys. 07 (2011) 025.
[45] J. Chluba and D. Jeong, Mon. Not. R. Astron. Soc. **438**, 2065 (2014).
[46] R. Khatri and R. A. Sunyaev, J. Cosmol. Astropart. Phys. 09 (2012) 016.
[47] J. Chluba, Mon. Not. R. Astron. Soc. **434**, 352 (2013).
[48] C. Destri, H. J. de Vega, and N. G. Sanchez, Phys. Rev. D **78**, 023013 (2008).
[49] T. Kobayashi and F. Takahashi, J. Cosmol. Astropart. Phys. 01 (2011) 026.
[50] A. R. Liddle, P. Parsons, and J. D. Barrow, Phys. Rev. D **50**, 7222 (1994).
[51] W. H. Kinney, Phys. Rev. D **66**, 083508 (2002).
[52] M. Zaldarriaga, L. Hui, and M. Tegmark, Astrophys. J. **557**, 519 (2001).
[53] P. Adshead, R. Easther, J. Pritchard, and A. Loeb, J. Cosmol. Astropart. Phys. 02 (2011) 021.
[54] N. Palanque-Delabrouille *et al.*, J. Cosmol. Astropart. Phys. 11 (2015) 011.
[55] N. Palanque-Delabrouille *et al.*, Astron. Astrophys. **559**, A85 (2013).